END
DATE
FILMED
|-81
DTIC

MICROCOPY RESOLUTION TEST CHART

BR74910
TR 80052

AD A091888

ROYAL AIRCRAFT ESTABLISHMENT

*

Technical Report 80052

April 1980

FEATURES OF THE UPPER ATMOSPHERE REVEALED BY ANALYSIS OF THE ORBIT OF COSMOS 1009 ROCKET, 1978-50B

by

H. Hiller

D.G. King-Hele

*

ROYAL AIRCRAFT ESTABLISHMENT

(6) FEATURES OF THE UPPER ATMOSPHERE REVEALED BY ANALYSIS OF THE ORBIT OF COSMOS 1009 ROCKET, 1978-50B

by

(10) H. Hiller
D. G. King-Hele

(12) 30

SUMMARY

Cosmos 1009 rocket was launched on 19 May 1978 into an orbit with initial perigee height 150 km and apogee 1100 km: its lifetime was only 17 days. The orbit has been determined daily during the final 14 days of its life, using the RAE orbit refinement program PROP6, with about 1100 observations supplied by NORAD. An average accuracy of about 60 m, radial and cross-track, was achieved.

The orbits were analysed to reveal three features of the upper atmosphere at heights between 125 and 175 km. From the decrease in perigee height, five values of density scale height, accurate to ±4%, were obtained. The first three were within 10% of those from *CIRA 1972*; the fourth, after a magnetic storm, was higher than expected; the fifth gave evidence of the decrease in drag coefficient at heights below 130 km.

Atmospheric oblateness produced a change of $4°$ in perigee position during the last four days of the life. Analysis showed that the ellipticity of the upper atmosphere was approximately equal to that of the Earth, f, for the first two of the four days, and about $\frac{1}{2}f$ in the last two.

The orbital inclination decreased during the 14 days by about 50 times its standard deviation, and the observed variation was analysed to determine zonal winds at heights of 150-160 km at latitudes near $47°$ north. The zonal wind was very weak (0 ± 30 m/s) for 23-28 May at local times near 03 h; and 90 ± 30 m/s east-to-west for 29 May to 4 June at local times near 01 h.

310450

2

LIST OF CONTENTS

1   INTRODUCTION

Cosmos 1009 rocket, 1978-50B, was launched on 19 May 1978 into a low-perigee orbit, the initial orbital parameters being approximately as follows: inclination 65.1°; perigee height 150 km; apogee height 1100 km; eccentricity 0.07; and period 97.4 minutes. The rocket remained in orbit for only 17 days, decaying on 5 June. About 1750 observations were kindly supplied by the North American Air Defense Command (NORAD), of which about 1100 were finally used to determine daily orbits during the final 14 days in orbit, with the aid of the RAE orbit refinement program[1], PROP6.

The orbit was chosen for analysis because its high drag offers the chance to determine upper-atmosphere properties at heights of 120-180 km at close intervals in time. Three distinct features of the upper atmosphere are investigated. The density scale height is determined from the changes in perigee height (sections 3 and 4). The oblateness of the atmosphere is assessed from the variation of the argument of perigee (section 5). The zonal wind is studied by analysing the decrease in orbital inclination (section 6).

2   THE ORBIT

About 1100 observations have been used to determine the orbits, from the 1750 supplied by the assigned and contributing sensors of the North American Air Defense Command (NORAD) Space Detection and Tracking Systems (SPADATS). Orbits have been determined daily during the last 14 days of the satellite's 17-day life, the epoch being at 00 h each day. Table 1 gives the orbital parameters.

Table 1 shows that the standard deviation in inclination, i , ranges from 0.0003 to 0.0013°; the sd in eccentricity, e , from 4×10^{-6} to 20×10^{-6}. These are equivalent to between 30 and 150 m in position for both i and e , and the average for both is 60 m. The sd in right ascension of the node, Ω , is between 0.0005 and 0.0013°; while for the argument of perigee, ω , and mean anomaly at epoch, M_0 , the sd varies in unison, the extremes being 0.005 and 0.054°. The largest sd of each orbital element applies to the final orbit (for the 18 h before decay). The inclination values, in Fig 1, show a strong decrease which is used to determine the atmospheric winds (section 6). The variations in semi major axis a and in e and Ω , Figs 2-4, follow the expected pattern. The only unusual feature is the 'turn-up' in ω near decay (Fig 5); this is discussed in section 5.

052

Table 1

Orbital parameters for Cosmos 1009 rocket, with standard deviation

Run	MJD	Date 1978	a	e	i	Ω	ω	M_0	M_1	M_2	M_3	M_4	ε	D	N
1	43651.0	May 23	6957.627	0.063371	65.1439	264.0704	56.030	48.857	5386.225	11.378	0.54		0.42	1.1	100
			2	8	4	10	10	9	3	9	2				
2	52.0	24	6937.875	0.060829	65.1436	260.9414	55.732	47.645	5409.248	10.869	0.12		0.20	0.7	66
			3	5	5	5	6	9	3	8	3				
3	53.0	25	6919.017	0.058352	65.1415	257.7852	55.353	67.857	5431.381	11.105	-		0.38	0.8	73
			1	9	5	10	10	9	1	8					
4	54.0	26	6900.247	0.055877	65.1403	254.5964	55.006	110.330	5453.562	10.617	-0.40		0.72	1.3	79
			2	9	5	10	14	14	3	3	2				
5	55.0	27	6881.681	0.053436	65.1385	251.3797	54.589	174.958	5475.651	10.778	0.30		0.39	0.6	97
			4	7	5	6	7	6	4	15	6				
6	56.0	28	6863.215	0.051004	65.1380	248.1340	54.208	261.655	5497.769	10.652	-0.35		0.47	1.3	97
			4	6	5	6	5	7	4	5	1				
7	57.0	29	6844.370	0.048404	65.1369	244.8607	53.931	10.054	5520.495	13.199	0.63		0.54	0.9	85
			4	10	6	13	12	11	4	19	4				
8	58.0	30	6821.479	0.045306	65.1357	241.5550	53.536	144.243	5548.312	14.766	1.90		0.46	0.6	86
			5	12	5	12	11	10	6	18	7				
9	59.0	31	6795.598	0.041983	65.1339	238.2060	53.247	308.193	5580.046	15.305	-0.96		0.54	1.1	77
			5	11	6	12	19	18	6	11	3				
10	60.0	Jun 1	6769.911	0.038490	65.1332	234.8140	52.977	143.396	5611.841	17.196	1.02		0.34	0.7	75
			3	5	6	6	9	8	4	7	4				
11	61.0	2	6740.850	0.034514	65.1286	231.3778	52.729	13.221	5648.178	18.151	3.55	5.05	0.46	0.8	93
			8	7	4	8	11	11	10	26	17	23			
12	62.0	3	6702.436	0.029114	65.1263	227.8751	53.220	282.740	5696.815	29.322	1.82	-1.02	0.60	1.5	55
			8	17	8	13	26	24	7	25	1	4			
13	63.0	4	6654.696	0.022920	65.1217	224.3075	53.534	249.151	5758.241	34.062	8.62		0.33	0.9	59
			5	4	7	5	29	28	7	18	4				
14	64.0	5	6573.513	0.012272	65.1153	220.6229	55.230	289.766	5865.265	108.056	112.50	86.2	0.62	0.7	55
			31	20	13	6	54	53	41	76	97	1.5			

KEY: MJD Modified Julian Day
  a   semi major axis (km)
  e   eccentricity
  i   inclination (deg)
  Ω   right ascension of node (deg)
  ω   argument of perigee (deg)

M_0 mean anomaly at epoch (deg)
M_1 mean motion, n (deg/day)
M_2–M_4 additional coefficients in polynomial for M
  ε   measure of fit
  D   time coverage of observations (days)
  N   number of observations used

3 VARIATION IN PERIGEE HEIGHT

Perigee height is evaluated first, as a prerequisite to finding the heights at which scale height, atmospheric oblateness and atmospheric rotation are being measured. The values of semi major axis, a , and eccentricity, e , given in Table 1, were used to calculate perigee height over a spherical Earth, h_p , from

$$h_p = a(1 - e) - R ,\qquad(1)$$

where R is the Earth's mean equatorial radius, 6378.14 km. These values of h_p are plotted as crosses with a mean curve through them, in Fig 6. The perturbations, Δe , in e due to zonal-harmonic and lunisolar effects were calculated from the PROD program[2], and used to obtain values of

$$Q = h_p + a\Delta e ,\qquad(2)$$

which should be free of gravitational perturbations. These values of Q are plotted, with a mean curve, in Fig 7. The slope $\dot{Q}$ of this curve is used to determine density scale height (section 4).

The perigee height, y_p , is obtained from (1) by adding the change due to the local Earth radius at perigee latitude to give, for inclination 65.1°,

$$y_p = h_p + 17.60 \sin^2\omega .\qquad(3)$$

The values of y_p , after a small adjustment for the dynamical effects of the Earth's oblateness[3], are plotted as circles in Fig 6, with a mean (broken) curve; since ω always remains between 52 and 56°, the two curves in Fig 6 are nearly parallel.

4 DENSITY SCALE HEIGHT

The density scale height H is a measure of the rate of decrease of density ρ as height y increases, and is defined by

$$\frac{1}{H} = -\frac{1}{\rho}\frac{d\rho}{dy} .\qquad(4)$$

If, as here, $ae/H > 3$, values of H can be calculated from $\dot{Q}$, the rate of change of Q due to air drag using the equation[4]

$$\dot{Q} = -\frac{H_1 \dot{M}_1}{3M_1 e}\left(1 - 2e + \frac{H_1}{4ae} - \frac{2\epsilon'}{e}\sin^2 i \cos 2\omega\right), \tag{5}$$

where ϵ' is the ellipticity of the atmosphere (taken equal to the ellipticity of the Earth, 0.00335) and H_1 applies at a height y_1, $1.5H_p$ above perigee height y_p. The remaining variables are given in Table 1.

Values of $\dot{Q}$ are obtained in the form $\Delta Q/\Delta t$, where ΔQ is the change in Q over a suitable time interval Δt. A change, ΔQ, of at least 3 km is required to ensure that the error in $\dot{Q}$ does not exceed 5 per cent and this determines the time interval Δt selected. Mean values of the variables of equation (4) are calculated for each time interval. In this way, five observational values of H_1 were obtained.

However, the method is not satisfactory for the last 2 days before decay, because the values of $\dot{M}_1$ and e change greatly between one orbit and the next, and the allocation of a mean value for use in equation (5) thus becomes subject to error, of a magnitude difficult to estimate. In these circumstances an integrated version of equation (5) is preferable. From equation (2) of Ref 4,

$$\frac{da}{dx} = 1 + \frac{H_1}{2x} - \frac{H_1}{a} + \left(\frac{3H_1}{8} - \epsilon' a \sin^2 i \cos 2\omega\right)\frac{H_1}{x^2}, \tag{6}$$

where $x = ae$. Taking a as constant ($= \bar{a}$) in the small terms on the right-hand side, taking $\cos 2\omega$ as constant, and integrating between x_0 and x_1, we have

$$(a_1 - x_1) - (a_0 - x_0) = \frac{H_1}{2}\ln\frac{x_1}{x_0} - \frac{H_1}{\bar{a}}(x_1 - x_0)$$
$$-\left(\frac{3H_1}{8} - \epsilon'\bar{a}\sin^2 i \cos 2\omega\right)\left(\frac{H_1}{x_1} - \frac{H_1}{x_0}\right). \tag{7}$$

If x_0 and x_1 are taken as the values of x at the beginning and end of the chosen time interval Δt, the left-hand side of equation (7) is ΔQ. The ln term on the right-hand side is the main term and we may write $a_1 = a_0 = \bar{a}$ in the smaller terms, so that equation (7) gives:

$$H_1 = \frac{(-\Delta Q)}{\frac{1}{2}\ln\frac{a_0 e_0}{a_1 e_1} - (e_0 - e_1) + \left(\frac{3H_1}{8\bar{a}} - \epsilon'\sin^2 i \cos 2\omega\right)\left(\frac{1}{e_1} - \frac{1}{e_0}\right)}, \tag{8}$$

where e_0 and e_1 should, strictly, be cleared of zonal harmonic and lunisolar perturbations, so that $e_0 = 1 - (R + Q_0)/a_0$, etc. For 1978-50B this effect was significant only for the final value of H_1.

It should be emphasized that equation (8) is preferable to equation (5) whenever (a) accurate values of e are available, *and* (b) the drag substantially reduces e during the chosen time interval, Δt. If e is not much reduced by drag, so that $e_0 \simeq e_1$, it is dangerous to use equation (8), and equation (5) is greatly to be preferred.

For the first three of the values of H_1, virtually identical results were obtained from equations (5) and (8); but for the last two values there were substantial differences, and the values from equation (8) are to be preferred in this situation for the reasons given above.

The five observational values of H_1 are plotted in Fig 8 as circles with a vertical error bar and a horizontal line to show the time over which the value applies. Also shown are the daily values of the geomagnetic planetary index Ap (plotted with a delay of 1 day), the height y_1, and values of H_1 obtained[5] from *CIRA 1972* for the appropriate height and exospheric temperature, T_∞. The *CIRA* values are shown as crosses. The first three values of H_1 are all slightly higher than the *CIRA* values, the mean difference being 6 per cent and the maximum 10 per cent. The last two values are, however, 16 and 25 per cent higher than indicated by *CIRA*, and it seems that the magnetic storm on 2 June 1978, with $Ap = 82$, had a much greater effect than is predicted by *CIRA*. The rms error in H_1 is calculated to be near 1 km for all values, as shown in Fig 8.

The high value of H_1 for 3 June from the orbital analysis can be attributed to the magnetic storm, but the high value on 4 June probably arises from a quite different effect – a change in the aerodynamic flow regime at perigee from free-molecule flow to transition flow. Between June 4.0 and June 5.0 the perigee height decreased from 135 km, where the mean free path of the molecules is 20 m, to 126 km, where the mean free path is 7 m. The length of Cosmos 1009 rocket is believed to be 8 m, and free-molecule flow applies[6] only when the mean free path is considerably greater than the dimensions of the satellite. So it cannot be assumed that free-molecule flow exists below about 135 km. In transition flow the drag coefficient may decrease to about half its free-molecule-flow value[7]. On the last day in orbit, therefore, the drag coefficient would be expected to decrease over a short arc of the orbit near perigee, and, since the orbital theory is developed on the assumption of a constant drag coefficient, the resulting decrease in drag would be misinterpreted by the theory as a decrease in the

density at perigee, which would be modelled as an increase in scale height. Thus the high value of H_1 on the last day represents a 'drag scale height' rather than a density scale height, and would be expected to exceed the value from *CIRA*.

The first four values of H_1 have also been plotted against height y_1 as crosses, in Fig 9, against a background of comparative density scale height curves for various exospheric temperatures, T_∞ obtained from *CIRA 1972*. Adjacent to each cross is a value of T_∞ in brackets, calculated using appropriate values of solar 10.7 cm radiation energy, $S_{10.7}$, and geomagnetic planetary index, with adjustments for semi-annual variations. During May and June 1978, the value of $S_{10.7}$ was near 140×10^{-22} W m^{-2} Hz^{-1}, *ie* solar activity was fairly high.

5 ASSESSMENT OF UPPER-ATMOSPHERE OBLATENESS

The argument of perigee ω usually changes steadily throughout a satellite's life, the J_2 gravitational perturbation being dominant. However, if ω is near 45° (or 135°, 225° or 315°), the oblateness of the atmosphere creates an asymmetry between the drag experienced when approaching perigee and the drag when departing from perigee, and this asymmetry has the effect of altering ω. The change in ω thus produced is too small to be accurately measured, except for satellites of very high drag, and a substantial departure of ω from its gravitational variation is usually only found during the last day or two in orbit. The only previous analysis of this effect[7] was for 1970-114F, for which the perigee height was 110 km, and the total change in ω was less than 1°. As Fig 5 shows, the effect is much larger for 1978-50B, the final value of ω being about 4° higher than if the normal decrease had continued. It should therefore be possible to assess the magnitude of the atmospheric ellipticity ϵ'.

For an orbit with $z = ae/H > 3$, the change in ω due to atmospheric oblateness is given by equation (8) of Ref 7 as

$$\frac{\Delta\omega}{\Delta t} = -\frac{\Delta\Omega}{\Delta t}\cos i - \frac{2\epsilon' \sin^2 i \sin 2\omega}{3T_d e^2}\left\{1 + \frac{K}{e} + 0\left(e, \frac{K^2}{e^2}, \frac{1}{z^2}\right)\right\}\frac{\Delta T_d}{\Delta t}, \quad (9)$$

where T_d is the orbital period expressed as a fraction of a day and $K = 3\epsilon' \sin^2 i \cos 2\omega$. The change $\Delta\Omega$ in Ω which appears in equation (9) is that due to atmospheric rotation, and equation (5) of Ref 7 shows that $\Delta\Omega \simeq \frac{1}{6}\Lambda \sin 2\omega \, \Delta T_d$, so that the first term on the right-hand side of equation (9) is always less than 1% of the second term.

Because of the difficulty of assigning a mean value of e over the last day or two of the satellite's life, equation (9) cannot be used as it stands but needs to be integrated. Equation (4.52) of Ref 8 indicates that

$$\frac{\Delta T_d}{\Delta t} = \dot{T} = -\frac{3e_0 T_0}{4t_L \alpha}\left\{1 + \frac{H}{2a_0 e_0 \alpha} + \text{smaller terms}\right\} \tag{10}$$

where $\alpha = \sqrt{1 - t/t_L}$ and t_L is the remaining lifetime after time t_0. To test the accuracy of equation (10) for 1978-50B, we have to use the integrated form of the equation,

$$\frac{T}{T_0} = 1 - \frac{3e_0}{2}(1 - \alpha) + \frac{3H}{4a_0}\ln \alpha + \text{smaller terms} . \tag{11}$$

Fig 10a shows the observational values of T/T_0 (with the initial value at MJD 43660.0, approximately $4\frac{1}{2}$ days before decay), and the variation given by equation (11), taking $t_L = 4.5$ days, which gives the best fit. The agreement is excellent in Fig 10, so the theory is validated for 1978-50B and the further result that

$$\frac{e}{e_0} = \alpha + \text{terms of } 0(0.003) \tag{12}$$

can also be utilized. Fig 10b shows that the decrease in e^2 is nearly linear, as predicted by (12), the slight increase in slope towards the end probably being caused by the increase in density after the magnetic storm on 2 June. On inserting $\dot{T}$ from (10) into (9) and writing $e/e_0 = \alpha = (1 - t/t_L)^{\frac{1}{2}}$, we have

$$\dot{\omega} = -\dot{\Omega}\cos i + \frac{\varepsilon' \sin^2 i \sin 2\omega}{2e_0 t_L}\left[\left(1 - \frac{t}{t_L}\right)^{-\frac{3}{2}} + \left(\frac{K}{e_0} + \frac{H}{2a_0 e_0}\right)\left(1 - \frac{t}{t_L}\right)^{-2}\right] . \tag{13}$$

Integration of (13), assuming $\sin 2\omega$, K and H are constant, gives

$$\omega - \omega_0 = -\Delta\Omega\cos i + \frac{\varepsilon' \sin^2 i \sin 2\omega}{e_0}\left[\left(1 - \frac{t}{t_L}\right)^{-\frac{1}{2}} - 1\right.$$
$$\left. + \left(\frac{K}{2e_0} + \frac{H}{4a_0 e_0}\right)\left\{\left(1 - \frac{t}{t_L}\right)^{-1} - 1\right\}\right] . \tag{14}$$

10

or, using (12),

$$\omega - \omega_0 = -\Delta\Omega \cos i + \frac{\varepsilon' \sin^2 i \sin 2\omega}{e_0}\left[\frac{e_0}{e} - 1 + \left(\frac{K}{2e_0} + \frac{H}{4a_0 e_0}\right)\left(\frac{e_0^2}{e^2} - 1\right)\right]. \quad (15)$$

To apply equation (15), the values of ω are first cleared of gravitational perturbations: the resulting values are plotted in Fig 11a as circles. Also shown in Fig 11a are curves of the variation of ω given by equation (15) for three values of the atmospheric ellipticity ε', namely 0.5f, 0.75f and f, where f is the Earth's ellipticity (0.00335). None of the three curves fits all the points, and the best fit is obtained by taking $\varepsilon' = f$ for the first 2 days, and $\varepsilon' = \frac{1}{2}f$ for the last 2 days, Fig 11b. This result suggests that the magnetic storm on 2 June 1978 had the effect of reducing the atmospheric ellipticity to half its normal value, and that this effect continued over the two days. A decrease in oblateness implies an increase in density at high latitudes, and this is one of the known effects of the events associated with a magnetic storm.

In view of this result, the last two values of scale height H_1 were recalculated with ε' taken as $\frac{1}{2}f$ in equation (8), but the change was not significant.

6   UPPER-ATMOSPHERE WINDS

The 14 observational values of inclination, given in Table 1, were cleared of lunisolar and geopotential perturbations using the PROD program[2] with numerical integration at 1-day intervals. Perturbations due to Earth and ocean tides are expected to be somewhat smaller than the standard deviations, and were ignored. The values of inclination cleared of perturbations are plotted in Figs 12 and 13: it is apparent that the variation of inclination is very well-defined, the dec. · being 0.03°, which is 50 times the average sd of the values.

The variation of inclination is affected both by the west-to-east atmospheric rotation rate Λ, and by the south-to-north rotation rate μ, and the theoretical variation of inclination was calculated for a series of values of Λ, with $\mu = 0$ and $\mu = -0.1$, using the RAE computer program ROTATM with daily integration steps between 23 May and 5 June.

Unfortunately, it happens that an increase of 0.1 in μ has nearly the same effect as a decrease of 0.1 in Λ, so it is not possible to exploit the full accuracy of the values: instead we have to give pairs of values of Λ and

μ which fit the variation. Assuming that μ is fixed, it is not possible to
fit the points with a single value of Λ , and a break has to be made at May 29.0.
Then, as Figs 12 and 13 show, excellent fittings are possible, for μ = 0 , with
Λ = 1.0 up to May 29.0, and Λ = 0.8 thereafter; or, for μ = -0.1 , with
Λ = 0.9 up to May 29.0, and Λ = 0.7 thereafter. If the value of μ were
accurately known, the error in Λ due to observational error would be about 0.05.

The meridional winds at the relevant heights (140-160 km) and latitude
(near 45° north) have been studied in detail by Amayenc[9], who determined the
steady component and the diurnal and semi-diurnal variations in years of high
solar activity (1971-2) for all four seasons. His results show that in summer
the steady component is small, probably about 10 m/s from north to south; the
diurnal component has an amplitude which decreases from 45 m/s at 160 km to
30 m/s at 140 km, with the maximum at 21 h local time; the semi-diurnal component
has an amplitude decreasing from 35 m/s at 160 km to 25 m/s at 140 km, with a
maximum at 20 h local time at 160 km, and 22 h local time at 140 km. For 1978-50B
these results indicate an average south-to-north wind of 17 m/s for 23-28 May
(height 160 km), and a north-to-south wind of 11 m/s for 29 May to 4 June (height
150 km). Since the likely errors in these values are probably about 15 m/s, both
these wind speeds can be regarded as small, and it seems reasonable to assume that
μ = 0 ± 0.05 (corresponding to ±24 m/s). Thus the fitting shown in Fig 12 is to
be preferred.

Accepting the fitting of Fig 12, we have Λ = 1.0 for 23-28 May and
Λ = 0.8 for 29 May to 4 June, with sd made up of 0.05 from the assumed error in
μ and 0.05 from observational error, ie a total sd of 0.07. The values apply
at a height $\frac{2}{3}H$ above perigee, ie 160 and 150 km respectively (on taking y_p
from Fig 6, and H from Fig 8). In terms of wind speeds, the results are as
shown in Table 2.

Table 2

Values of zonal wind speed obtained

Date	Latitude	Local time	Height	East-to-west wind	Solar $S_{10.7}$ index	Geomagnetic conditions
1978 May 23-28	48°N	03 h	160 km	0 ± 30 m/s	145	Quiet
May 29-June 4	47°N	01 h	150 km	90 ± 30 m/s	135	Disturbed

The latitudes, local times and heights quoted are of course 'central' values: the wind is sampled over latitudes between about $40°$ and $55°$N, local times vary by up to ± 2 h and heights by up to ± 5 km from the values given.

These results need to be set in perspective in relation to other results. At heights between 120 and 160 km the most numerous measurements of zonal winds are those made by measuring the motion of vapour trails released from rockets, which reveal great variability with height[10,11], and a probable dependence on most of the other five parameters specified in Table 2, namely, season, latitude, local time, solar activity and geomagnetic conditions. It is also likely that the winds at these heights are influenced by irregular disturbances in the lower atmosphere, such as weather systems, thunderstorms, etc[12].

The zonal wind speeds found from incoherent radar scatter measurements, in conjunction with theoretical models, extend down to 130 km, but do not adequately reflect the known variability of the winds with height at the lower levels. Results by this technique for mid latitudes $(39-45°)$ in summer are given in Refs 13-15; and all indicate considerable changes in zonal winds as local time changes from 00 to 04 h, with eastward flow at 00 h and westward flow at 04 h. The time of zero wind is somewhat variable, but usually between 02 h and 03 h, which is consistent with the first line of Table 2; the second line of Table 2 does not show the west-to-east wind which is 'normal' at 01 h, no doubt because of the occurrence of the geomagnetic storm, which is quite enough to disrupt the normal pattern. (It is, of course, possible that the meridional wind may also be disturbed: if so, the resulting wind is likely to be from north to south, and Fig 13 would then apply, *ie* the zonal wind would still be from east to west, but stronger.)

There are no directly comparable results from satellite orbit analysis. The values at heights near 150 km obtained by Forbes[16] showed the strong influence of geomagnetic disturbances at latitudes of $45-75°$ north, but were all for local times of 10-13 h. The eight values of zonal wind found by King-Hele[17] from 1969-108A at heights near 160 km also showed the effect of geomagnetic disturbance, and indicated great variability with local time. The only one of the eight values at a relevant local time is for 02-05 h at 160 km height, and gives $\Lambda = 0.8$; but it is for equinox and for a lower latitude, $20°$ north.

7   CONCLUSIONS

The orbit of Cosmos 1009 rocket has been determined at daily epochs during the final 14 days of its 17-day life, from about 1100 observations supplied by

the North American Air Defense Command NORAD. Though the orbit was of extremely high drag, with the apogee height decreasing by 1000 km in 17 days, the perigee height and inclination were determined with an average accuracy equivalent to 60 m.

Three features of the upper atmosphere have been studied. The first is the density scale height. Five values were calculated from the rate of decrease of perigee height, and were compared with values obtained from the *CIRA 1972* Reference Atmosphere[5]. The first three observational values are all within 10% of the *CIRA* values, their mean value being 6% higher than *CIRA*. The fourth value is 16% higher than *CIRA:* this applies for the day after a magnetic storm, which seems to have had a greater effect than *CIRA* predicts. The fifth value applies for the last day in orbit when the perigee height decreased below 130 km, and the drag at perigee is reduced by the change from free-molecule to transition flow. The quantity measured is then a 'drag scale height', which should (and does) exceed the density scale height, being 25% higher than the value indicated by *CIRA*.

The oblateness of the upper atmosphere produced a change of 4° in the argument of perigee during the final 4 days of the satellite's life, and this perturbation has been analysed to obtain values of the atmospheric ellipticity ϵ' . The best fit is obtained by taking ϵ' equal to the ellipticity f of the Earth (0.00335) in the first 2 days, and $\epsilon' = \frac{1}{2}f$ during the last 2 days (June 3.0 to June 5.0). Evidently the magnetic storm on 2 June substantially reduced the atmospheric oblateness, presumably by increasing the density at high latitudes.

The decrease in orbital inclination is very well determined (see Fig 12) and (if the meridional wind is weak, as expected) the observed decrease implies very weak zonal winds (0 ± 30 m/s) at 160 km height for 23-28 May, and an east-to-west wind of 90 ± 30 m/s at 150 km for May 29 to June 4, when a geomagnetic storm occurred. Both results apply for latitude 40-50°N, and for local times near 03 h and 01 h respectively. These results are compared with values obtained by other techniques in section 6.

052

14

REFERENCES

No.	Author	Title, etc
1	R.H. Gooding R.J. Tayler	A PROP 3 users' manual. RAE Technical Report 68299 (1968)
2	G.E. Cook	Basic theory for PROD, a program for computing the development of satellite orbits. *Celestial Mechanics*, 7, 301-314 (1973) RAE Technical Report 71007 (1971)
3	Y. Kozai	The motion of a close Earth satellite. *Astronom. J.*, 64, 367-377 (1959)
4	D.G. King-Hele D.M.C. Walker	Air density at heights near 150 km in 1970, from the orbit of Cosmos 316 (1969-108A). *Planet. Space Sci.*, 19, 1637-51 (1971) RAE Technical Report 71129 (1971)
5	-	*CIRA 1972* (Cospar International Reference Atmosphere 1972). Akademie-Verlag, Berlin (1972)
6	G.E. Cook	Satellite drag coefficients. *Planet. Space Sci.*, 13, 929-946 (1965) RAE Technical Report 65005 (1965)
7	D.G. King-Hele	Analysis of the orbit of 1970-114F in its last 20 days. *Planet. Space Sci.*, 24, 1-16 (1976) RAE Technical Report 75088 (1975)
8	D.G. King-Hele	*Theory of satellite orbits in an atmosphere.* Butterworths, London (1964)
9	P. Amayenc	Tidal oscillations of the meridional neutral wind at midlatitudes. *Radio Science*, 9, 281-293 (1974)
10	J.F. Bedinger	Thermospheric motions measured by chemical releases. *Space Research XII* (Akademie Verlag, Berlin, 1972), pp 919-934
11	J.F. Bedinger H. Knaflich E. Manring D. Layzer	Upper-atmosphere winds and their interpretation. *Planet. Space Sci.*, 16, 159-193 (1968)

REFERENCES (concluded)

No.	Author	Title, etc
12	C.J. Rice L.R. Sharp	Neutral atmospheric waves in the thermosphere and tropospheric weather systems. *Geophys. Res. Letters,* 4, 315-318 (1977)
13	D.A. Antoniadis	Thermospheric winds and exospheric temperatures from incoherent scatter radar measurements in four seasons. *Journ. Atmos. Terr. Phys.,* 38, 187-195 (1976)
14	G. Hernandez R.G. Roble	Direct measurements of nighttime thermospheric winds and temperatures. 1. Seasonal variations during geomagnetic quiet periods. *Journ. Geophys. Res.,* 81, 2065-2074 (1976)
15	R.G. Roble J.E. Salah B.A. Emery	The seasonal variation of the diurnal thermospheric winds over Millstone Hill during solar cycle maximum. *Journ. Atmos. Terr. Phys.,* 39, 503-511 (1977)
16	J.M. Forbes	Wind estimates near 150 km from the variation in inclination of low-perigee satellite orbits. *Planet. Space Sci.,* 23, 726-731 (1975)
17	D.G. King-Hele	Analysis of the orbit of Cosmos 316 (1969-108A). *Proc. Roy. Soc. A,* 330, 467-494 (1972) RAE Technical Report 72062 (1972)
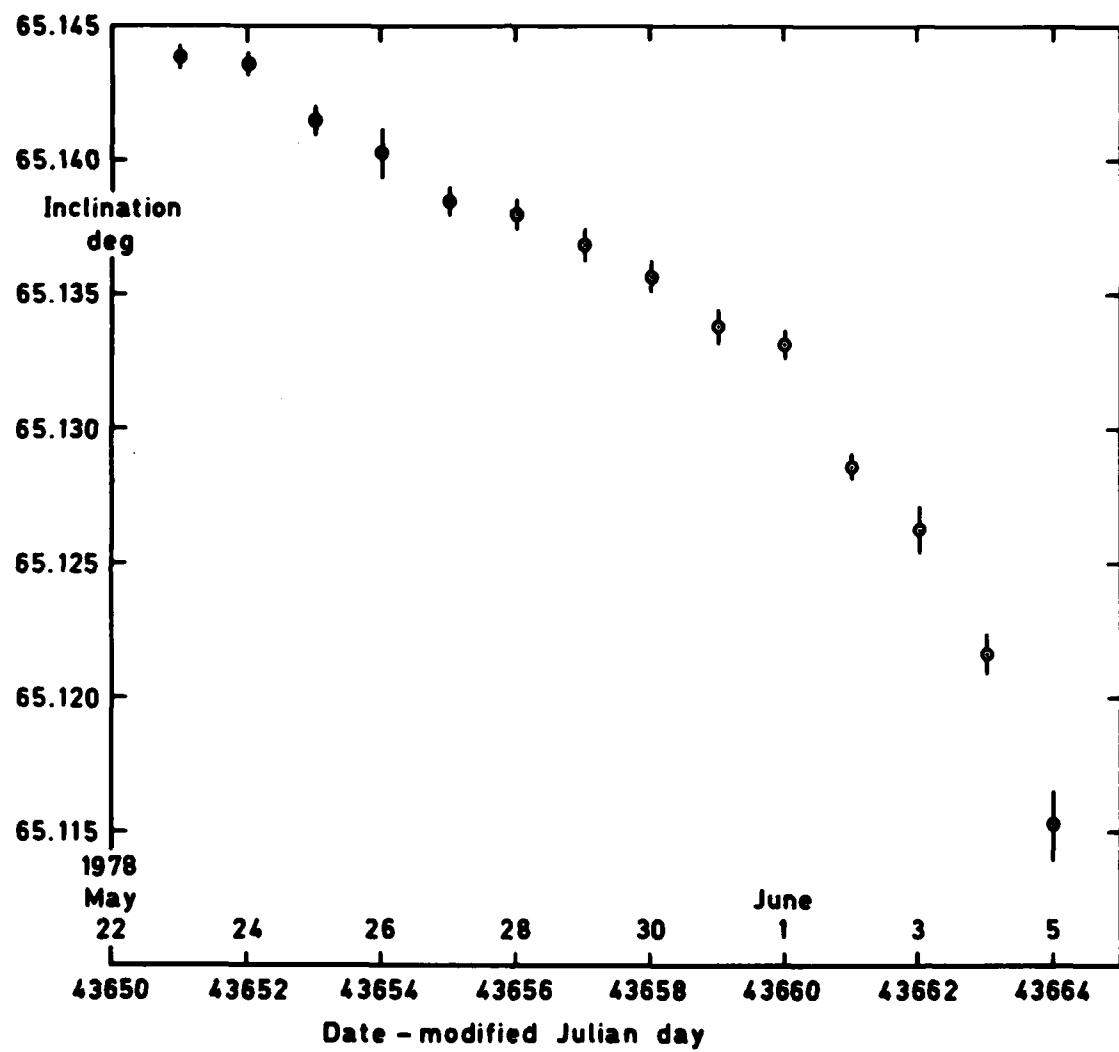
Fig 1

Fig 1   Observational values of inclination, with sd, for Cosmos 1009 rocket

Fig 2

Fig 2   Observational values of semi major axis, a
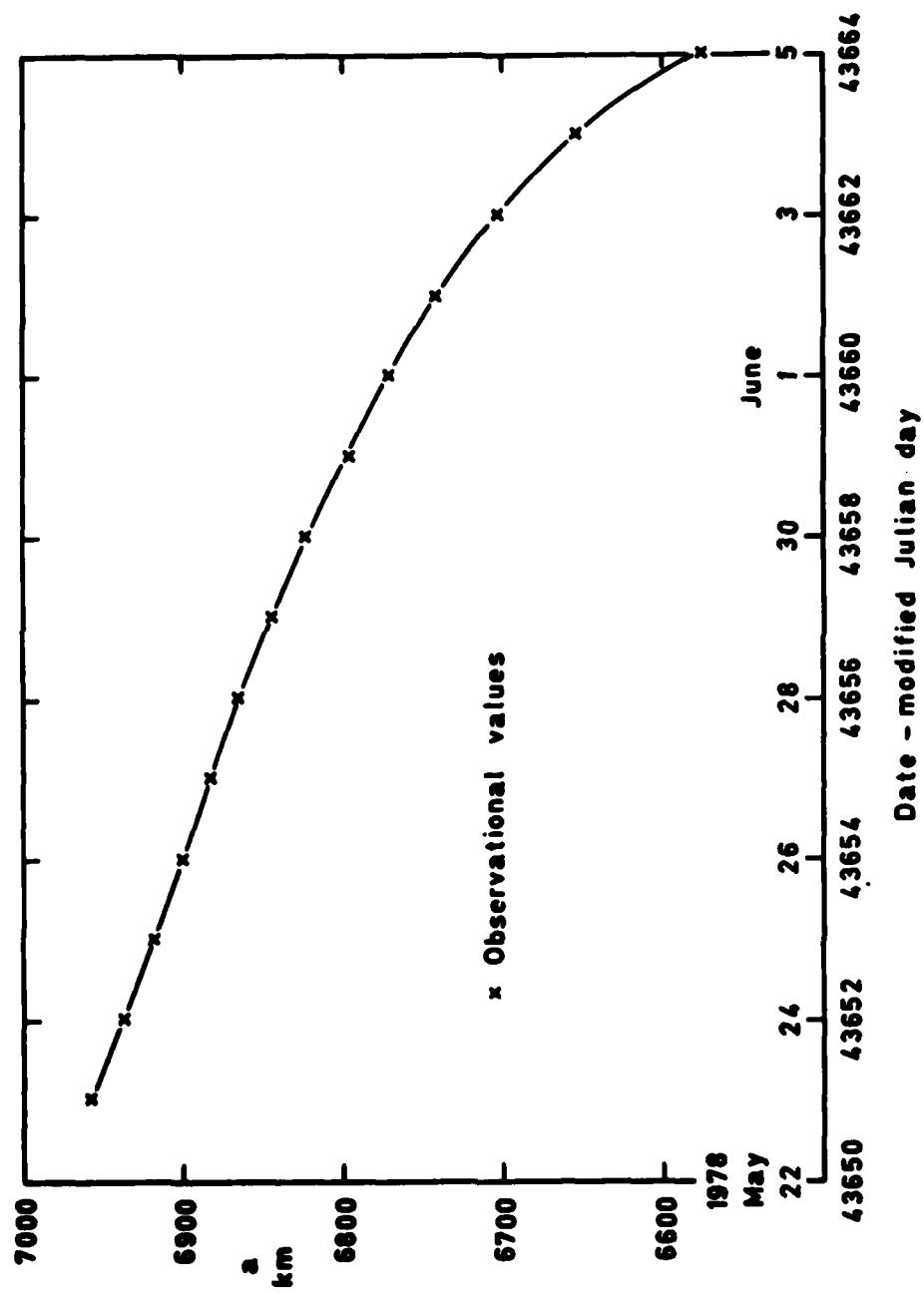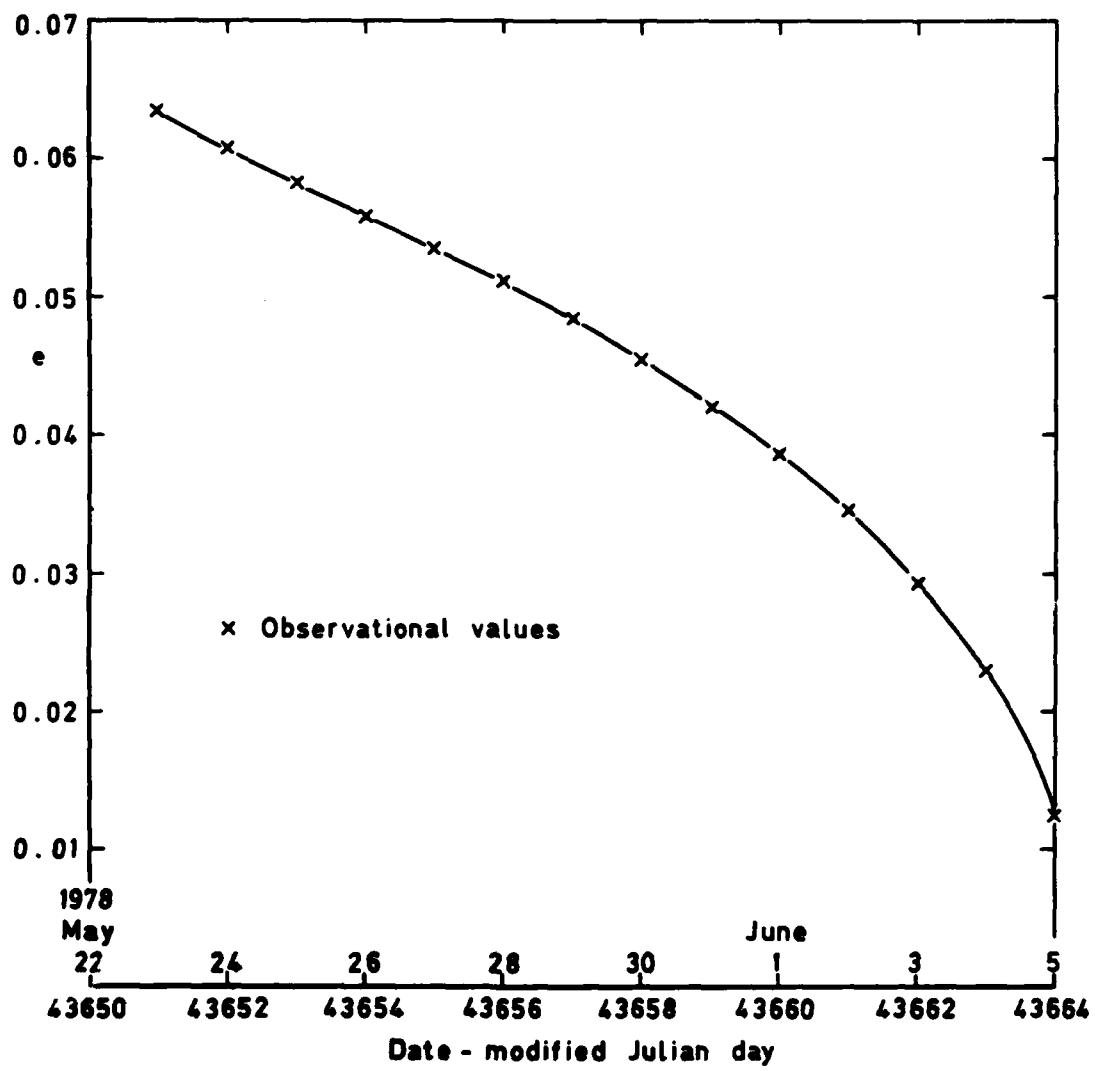
Fig 3

Fig 3 Observational values of eccentricity, e

Fig 4
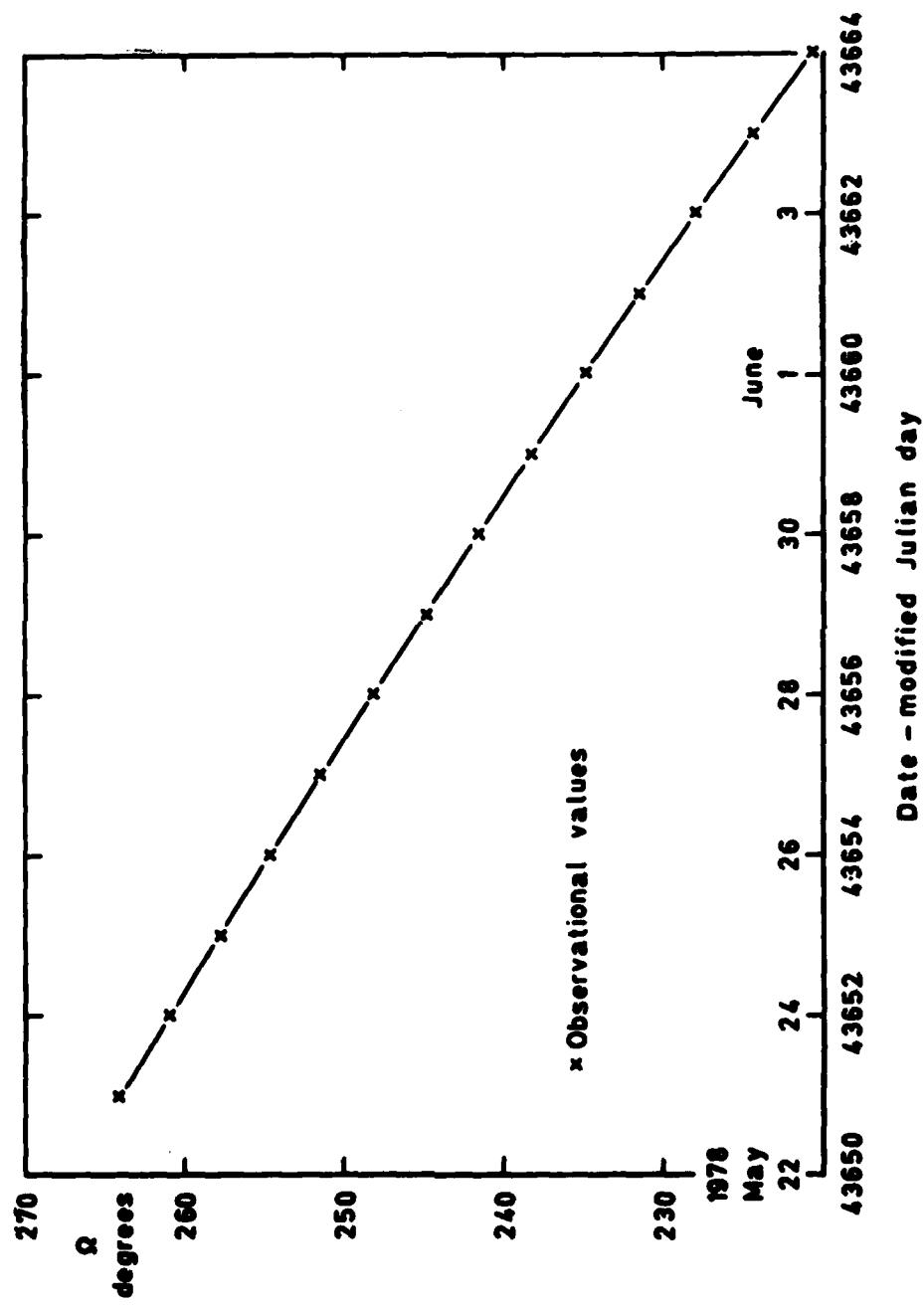
Fig 4 Observational values of right ascension of the node, Ω.

Fig 5

Fig 5   Observational values of argument of perigee, ω, with mean curve
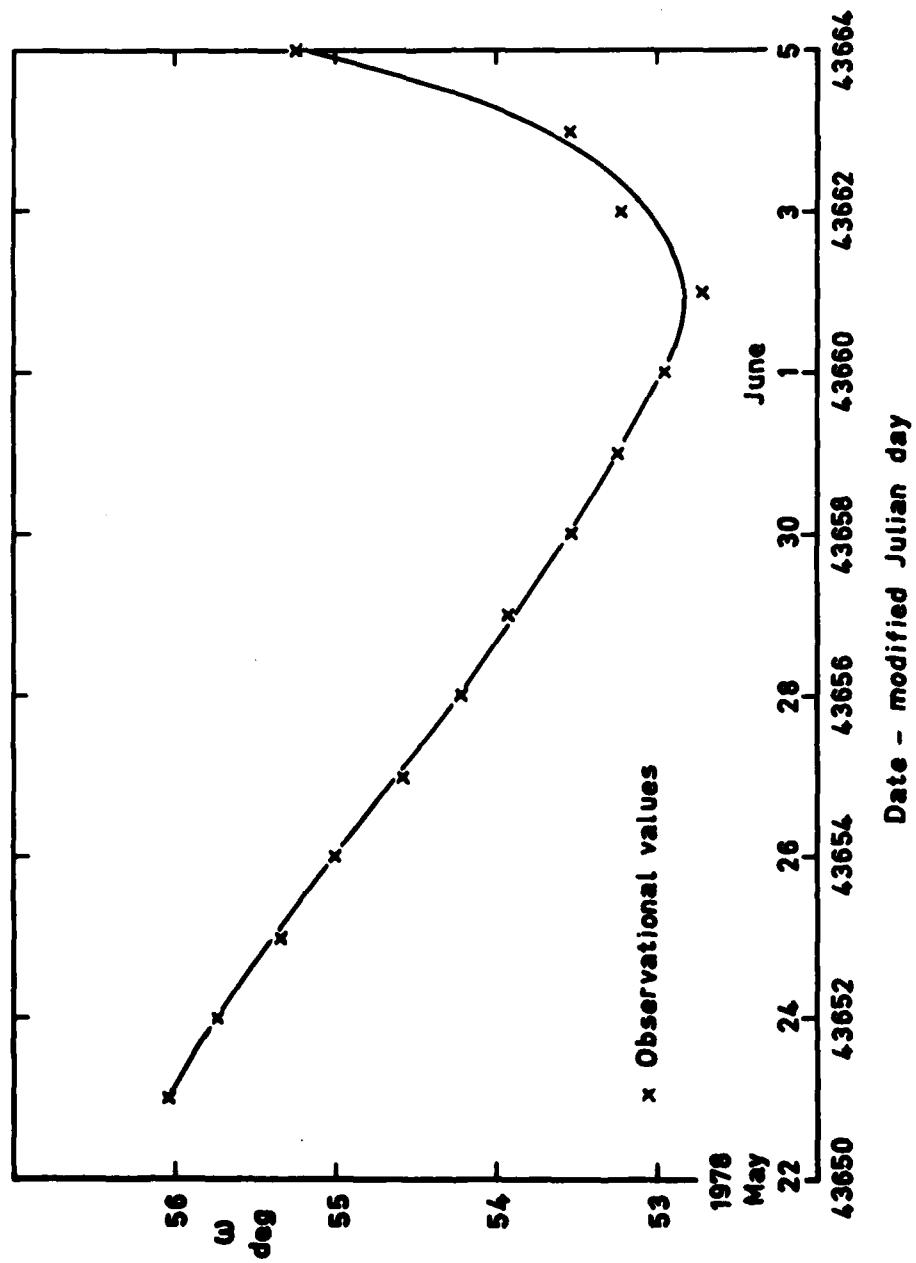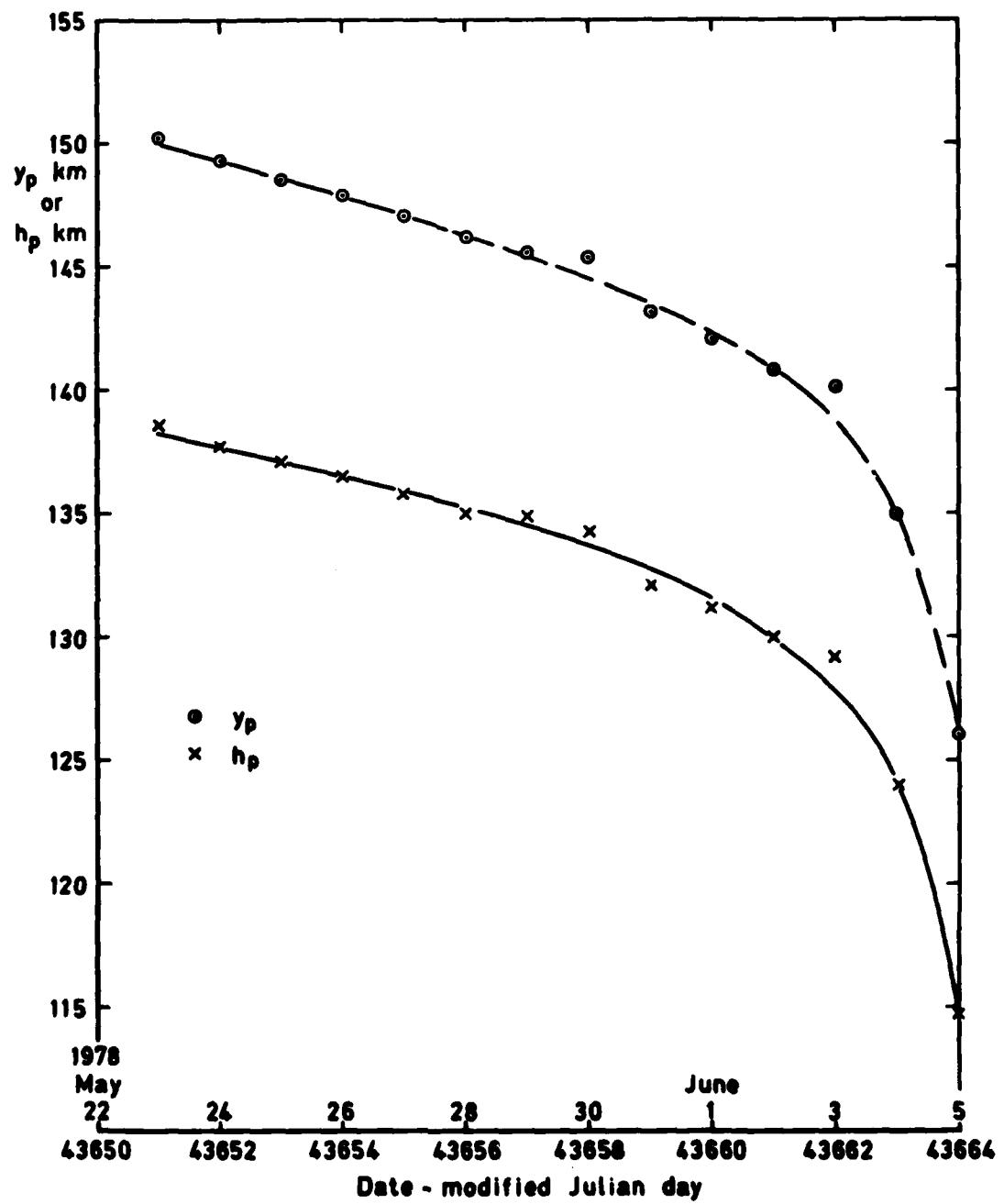
Fig 6

Fig 6   Perigee heights h_p (over spherical Earth) and y_p (over oblate Earth)

Fig 7
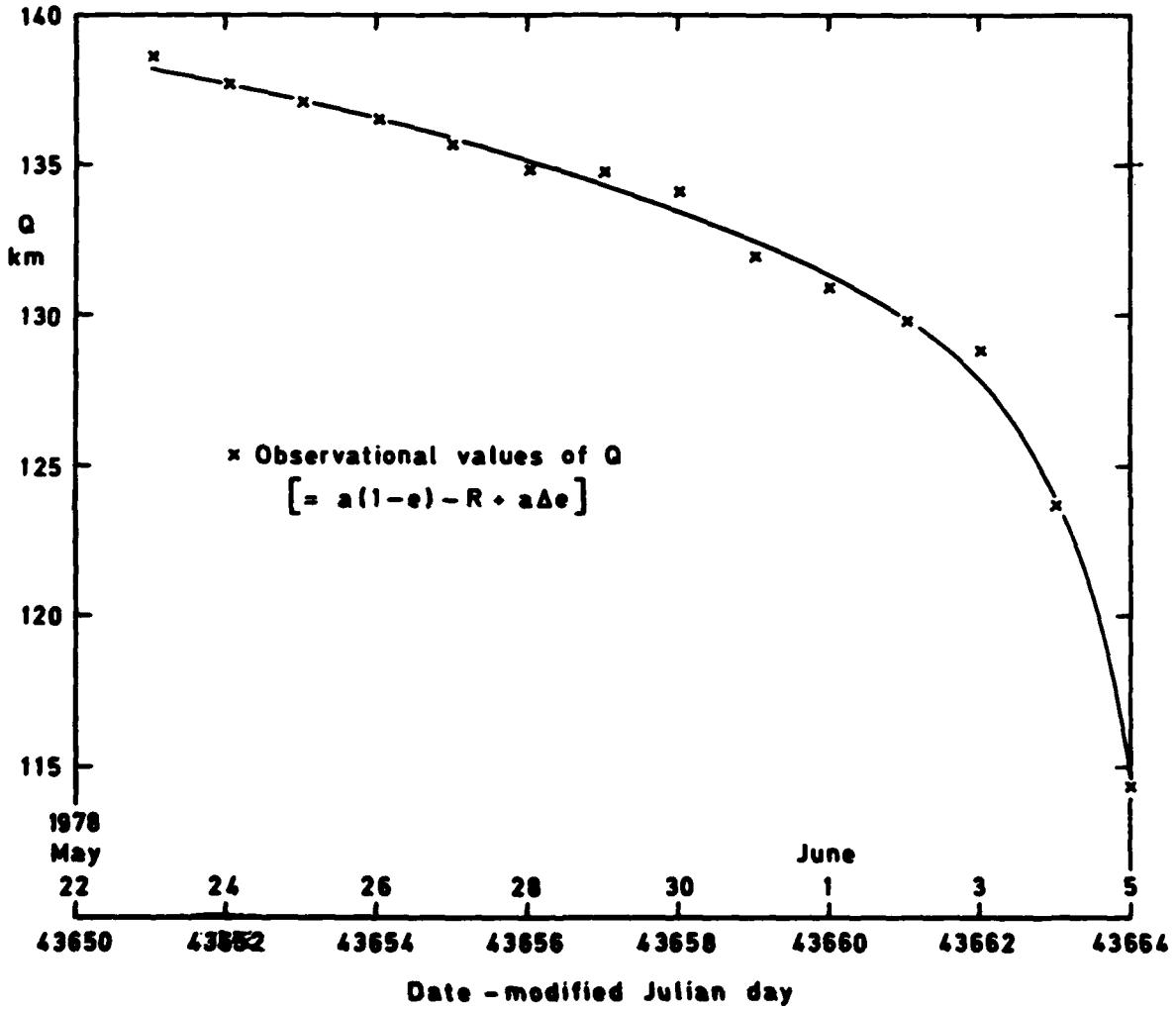
Fig 7   Values of perigee height, Q, cleared of gravitational perturbations

Fig 8
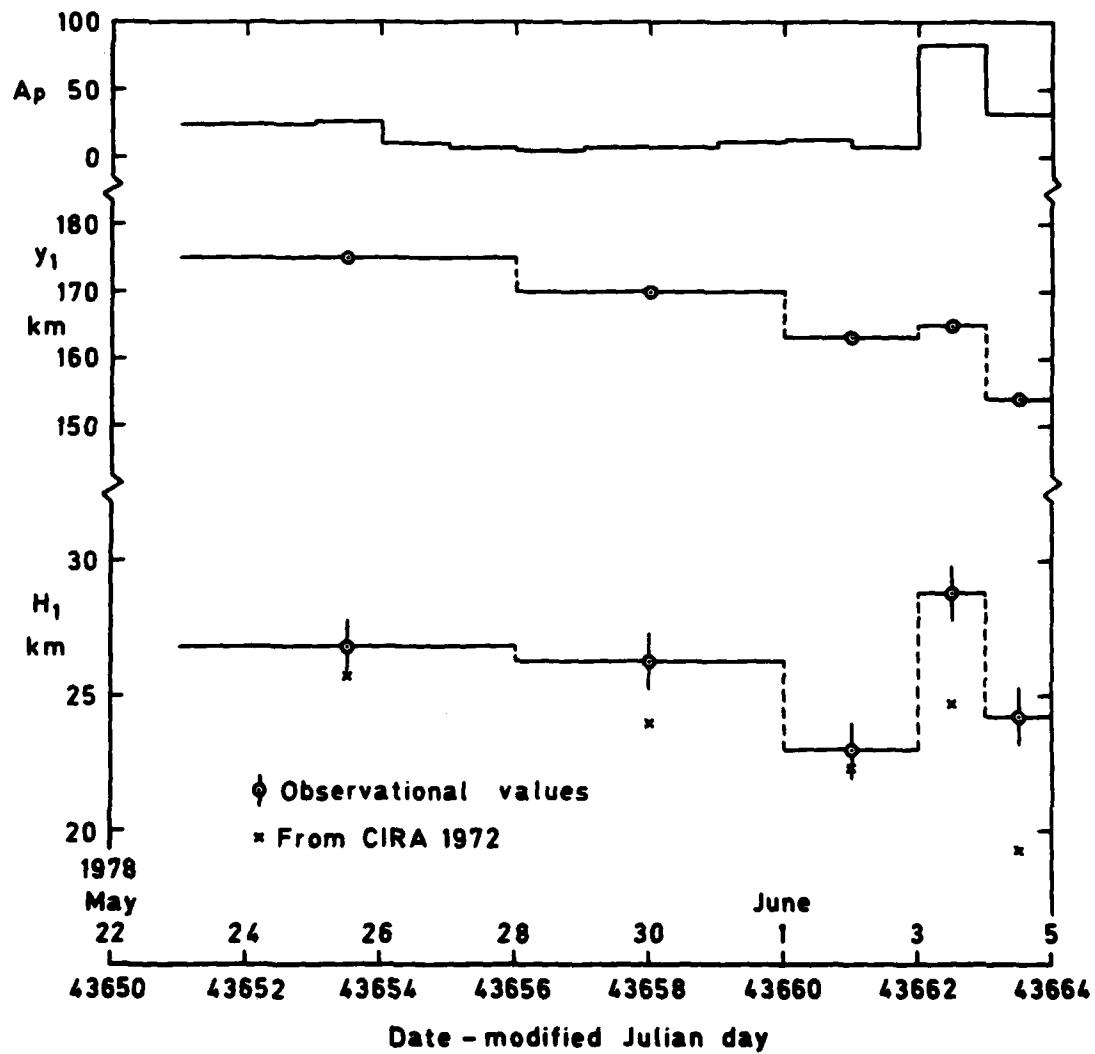
Fig 8   Scale height H_1, its height of application y_1, and geomagnetic planetary index, A_p

Fig 9
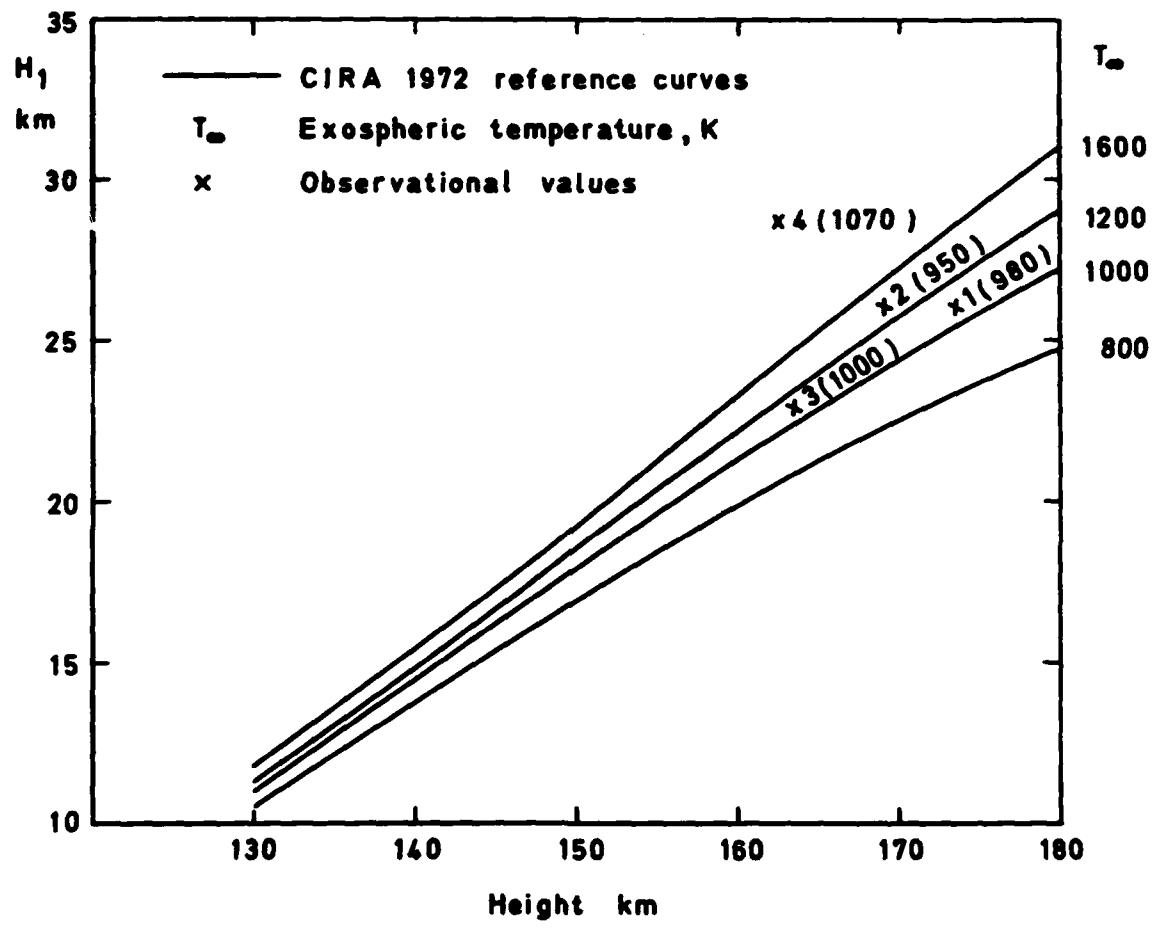
Fig 9   Values of density scale height, H_1, compared with CIRA 1972 curves

Fig 10

b Values of e^2, showing near-linear variation

a Values of T, with theoretical curve
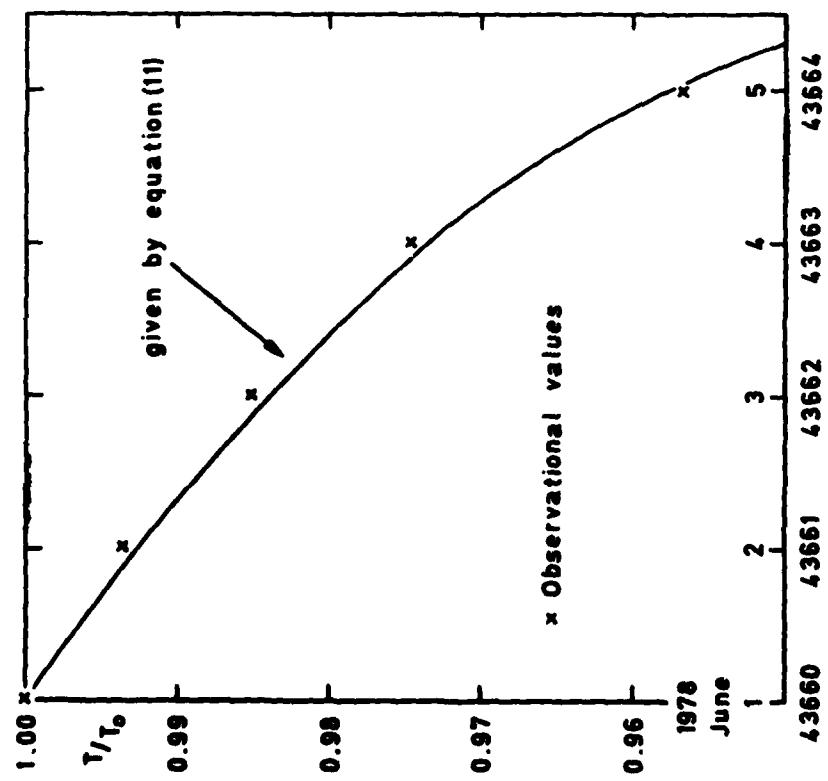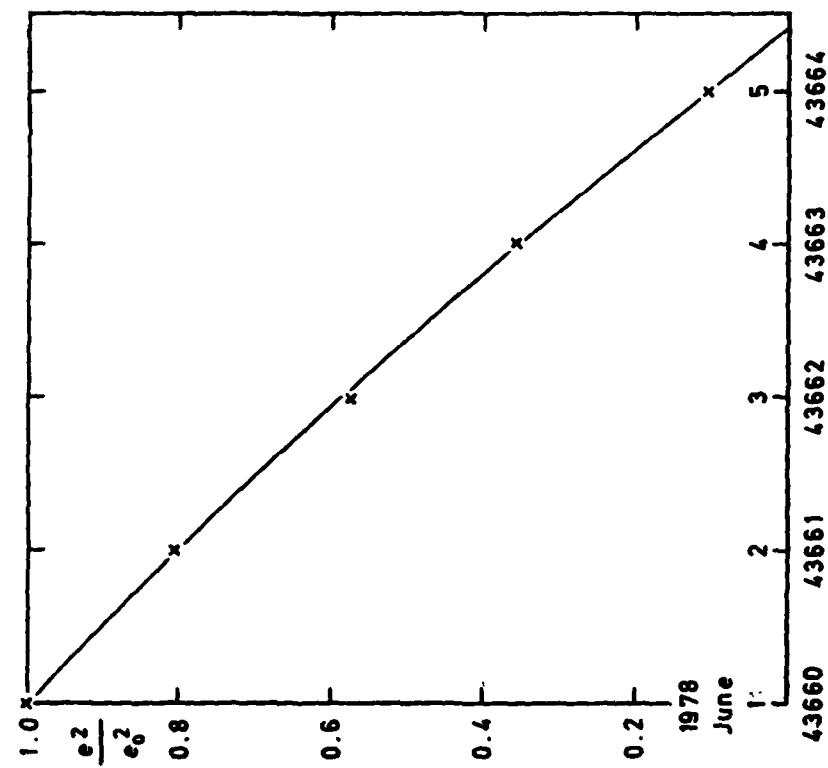
Fig 10a&b Values of orbital period T and eccentricity e in the four days before decay

Fig 11

a   With three fixed values of ϵ^{I}
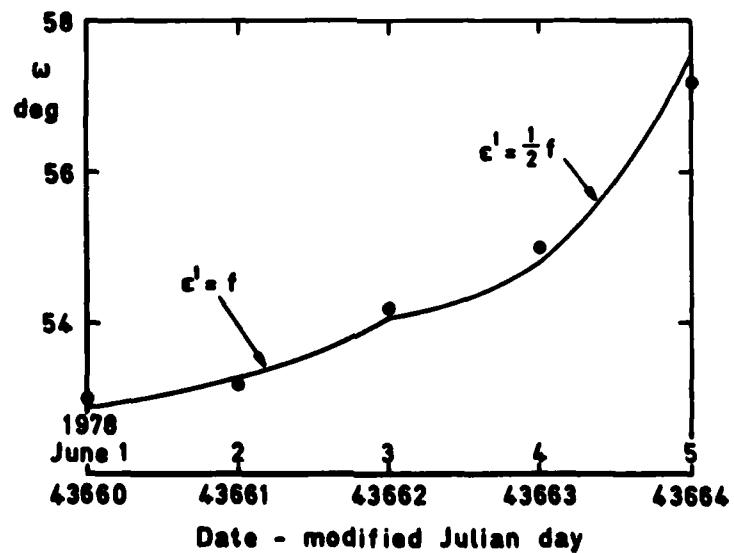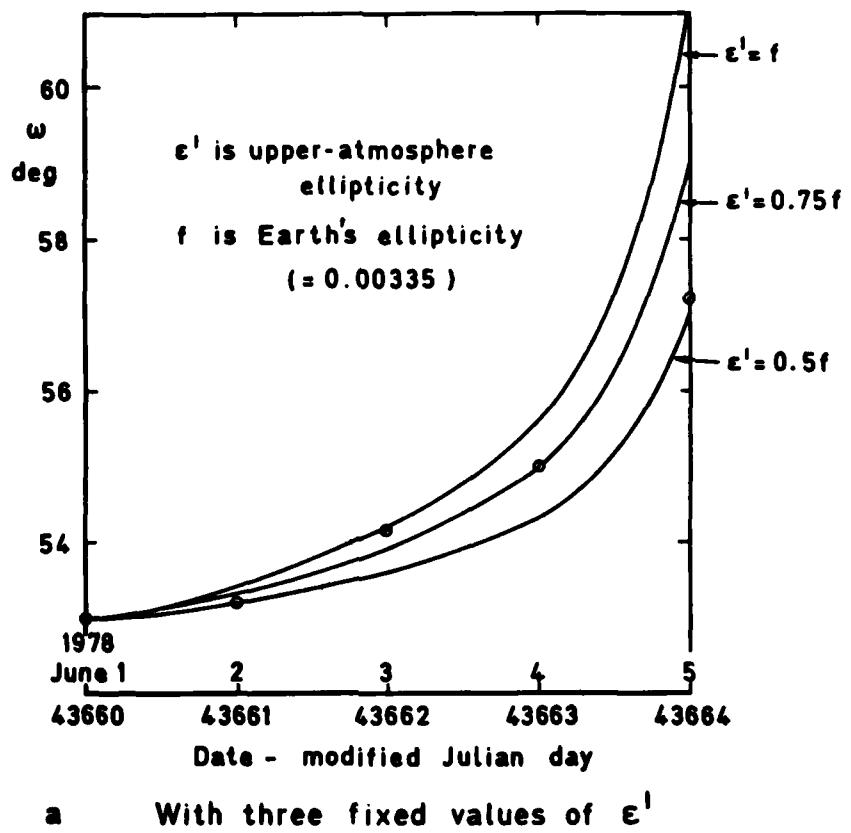
b   With values of ϵ^{I} to fit the observational values

Fig 11a&b   Argument of perigee cleared of gravitational perturbations, with theoretical curves for the effect of atmospheric oblateness, equation (15)

Fig 12
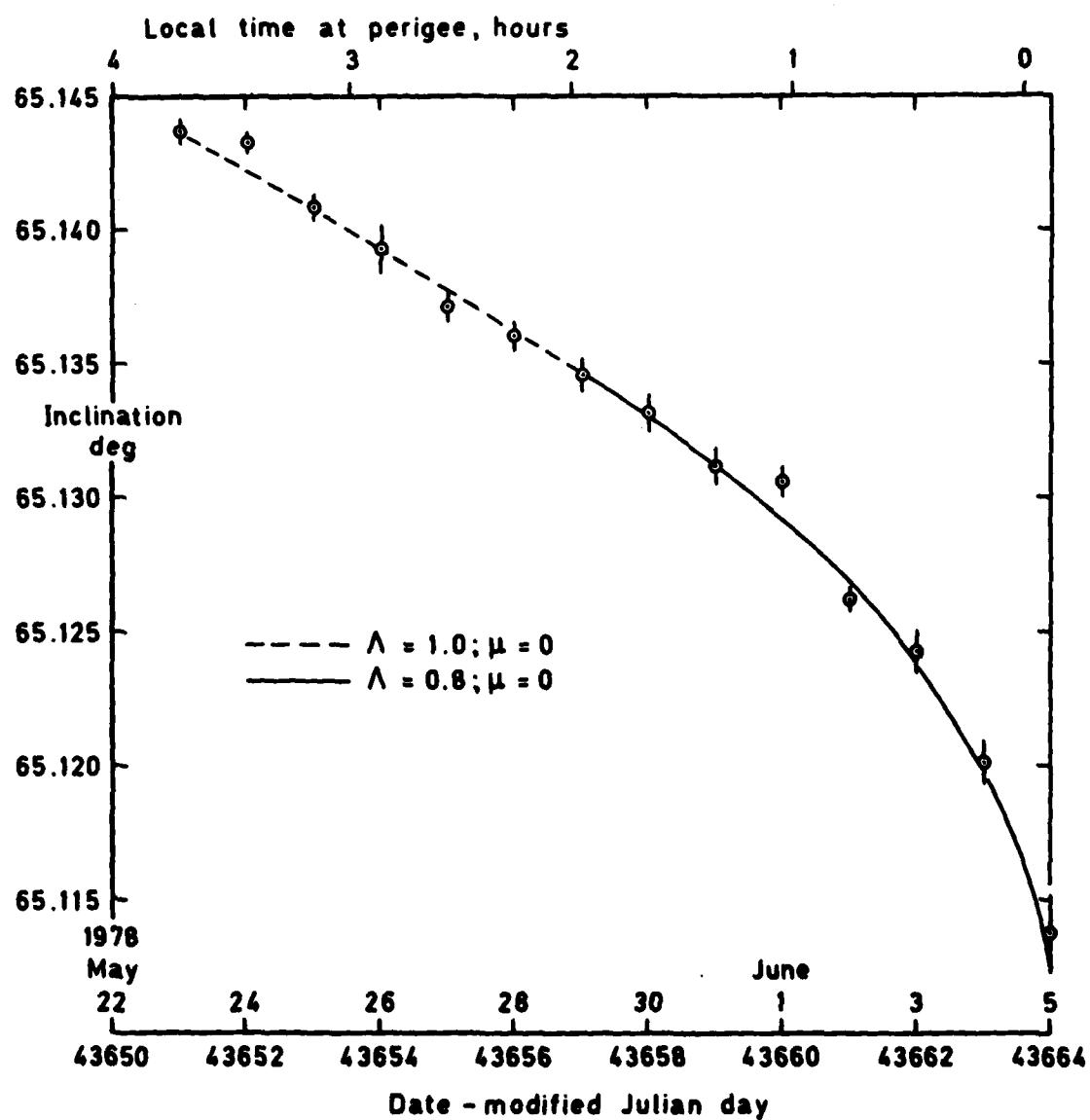
Fig 12   Inclination values with fitted Λ-curves (μ = 0)
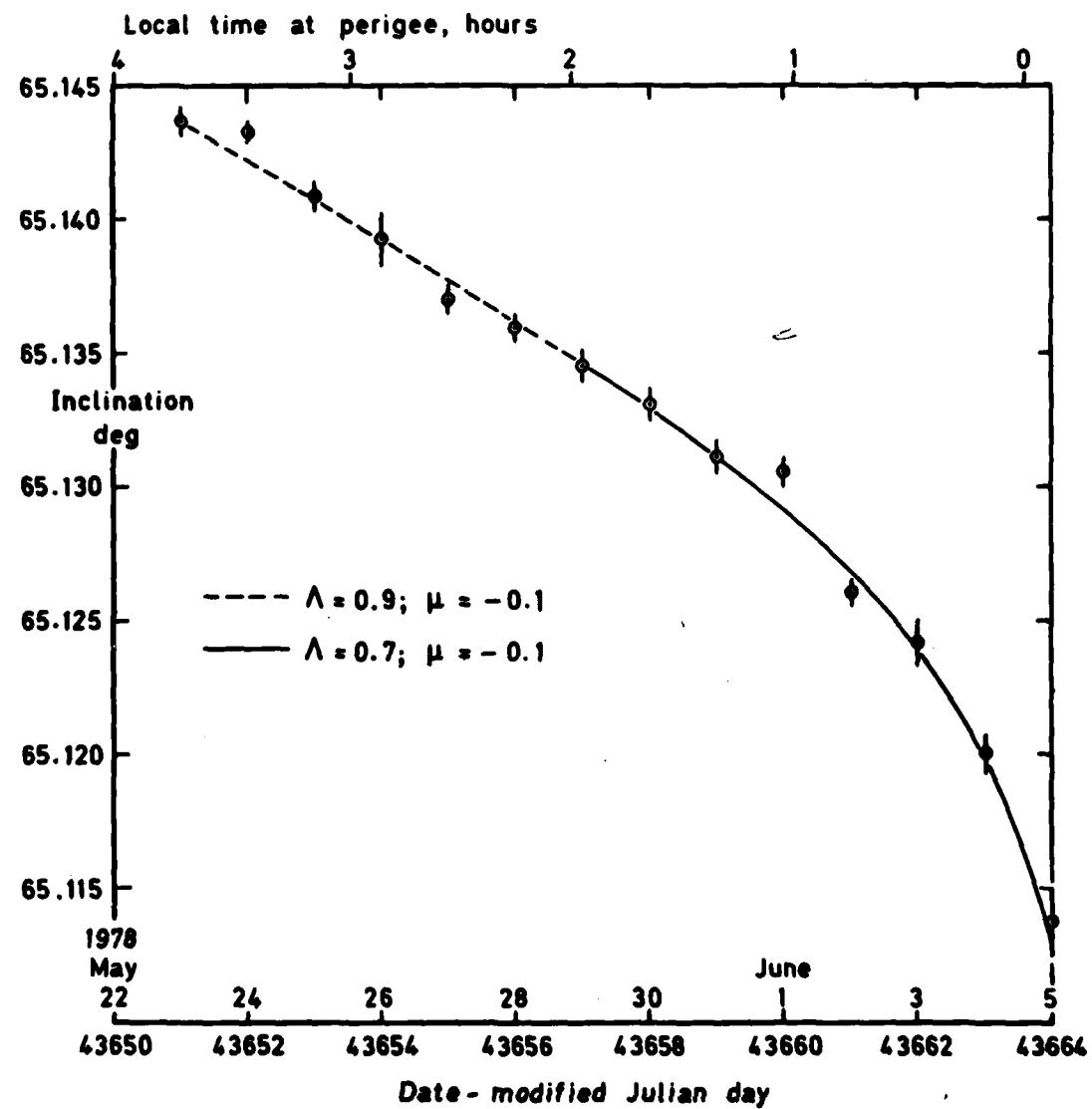
Fig 13

Fig 13   Inclination values with fitted Λ-curves (μ = 0)

REPORT DOCUMENTATION PAGE

Overall security classification of this page

UNLIMITED

Instructions for completion appear overleaf.

As far as possible this page should contain only unclassified information. If it is necessary to enter classified information, the box above must be marked to indicate the classification, e.g. Restricted, Confidential or Secret.

1. DRIC Reference (to be added by DRIC)	2. Originator's Reference RAE TR 80052	3. Agency Reference N/A	4. Report Security Classification/Marking UNLIMITED UNCLASSIFIED

5. DRIC Code for Originator 7673000W	6. Originator (Corporate Author) Name and Location Royal Aircraft Establishment, Farnborough, Hants, UK

5a. Sponsoring Agency's Code N/A	6a. Sponsoring Agency (Contract Authority) Name and Location N/A

7. Title Features of the upper atmosphere revealed by analysis of the orbit of Cosmos 1009 rocket, 1978-50B

7a. (For Translations) Title in Foreign Language

7b. (For Conference Papers) Title, Place and Date of Conference

8. Author 1. Surname, Initials Hiller, H.	9a. Author 2 King-Hele, D.G.	9b. Authors 3, 4	10. Date April 1980	Pages 28	Refs. 17

11. Contract Number N/A	12. Period N/A	13. Project	14. Other Reference Nos. Space 579

15. Distribution statement

(a) Controlled by – Head of Space Department, RAE (RAL)

(b) Special limitations (if any) –

16. Descriptors (Keywords) (Descriptors marked * are selected from TEST)

Upper atmosphere. Orbits. Cosmos 1009. Orbit decay. Atmospheric winds. Atmospheric oblateness.

17. Abstract

Cosmos 1009 rocket was launched on 19 May 1978 into an orbit with initial perigee height 150 km and apogee 1100 km: its lifetime was only 17 days. The orbit has been determined daily during the final 14 days of its life.

The orbits were analysed to reveal three features of the upper atmosphere at heights between 125 and 175 km. From the decrease in perigee height, five values of density scale height, accurate to 4%, were obtained. Atmospheric oblateness produced a change of 4 in perigee position during the last four days of the life. Analysis showed that the ellipticity of the upper atmosphere was approximately equal to that of the Earth, f, for the first two of the four days, and about $\frac{1}{2}f$ in the last two.

The orbital inclination was analysed to determine zonal winds at heights of 150-160 km at latitudes near 47 north. The zonal wind was very weak (0 ± 30 m/s) for 23-28 May at local times near 03 h; and 90 ± 30 m/s east-to-west for 29 May to 4 June at local times near 01 h.